



01 Jan 1992

## Electrical Conductivity And Seebeck Coefficient Of (La, Ca) (Cr, Co)<sub>03</sub>

R. Koc

Harlan U. Anderson

*Missouri University of Science and Technology*, harlanua@mst.edu

Follow this and additional works at: [https://scholarsmine.mst.edu/matsci\\_eng\\_facwork](https://scholarsmine.mst.edu/matsci_eng_facwork)

 Part of the [Materials Science and Engineering Commons](#)

---

### Recommended Citation

R. Koc and H. U. Anderson, "Electrical Conductivity And Seebeck Coefficient Of (La, Ca) (Cr, Co)<sub>03</sub>," *Journal of Materials Science*, vol. 27, no. 20, pp. 5477 - 5482, Springer, Jan 1992.

The definitive version is available at <https://doi.org/10.1007/BF00541609>

This Article - Journal is brought to you for free and open access by Scholars' Mine. It has been accepted for inclusion in Materials Science and Engineering Faculty Research & Creative Works by an authorized administrator of Scholars' Mine. This work is protected by U. S. Copyright Law. Unauthorized use including reproduction for redistribution requires the permission of the copyright holder. For more information, please contact [scholarsmine@mst.edu](mailto:scholarsmine@mst.edu).

# Electrical conductivity and Seebeck coefficient of (La, Ca) (Cr, Co)O<sub>3</sub>

R. KOC

*Middle East Technical University, Metallurgical Engineering Department, Ankara 06531, Turkey*

H. U. ANDERSON

*University of Missouri — Rolla, Ceramic Engineering Department, Rolla, MO 65401, USA*

Electrical conductivity and Seebeck coefficients of (La, Ca) (Cr, Co)O<sub>3</sub> were measured as a function of temperature. The electrical conductivity as measured in air from 100 to 1100 °C increased with increasing Co and Ca content. The Seebeck coefficients were positive, indicating p-type conductivity. The substitution of Co for Cr significantly decreased the Seebeck coefficients, indicating that the substitution resulted in an increase in site occupancy, associated with the Co. The additional Ca substitution for La resulted in further decrease in the Seebeck coefficients, then exhibited a temperature-independent behaviour, indicating that the carrier mobility, rather than carrier concentration, was thermally activated. The activation energies were 0.18 and 0.25 eV for LaCrO<sub>3</sub> and LaCoO<sub>3</sub>, respectively, and increased to about 0.50 eV with substitution of 10 mol % Co for Cr and then linearly decreased as Co content increased.

## 1. Introduction

The search for materials that possess the chemical stability and electrical conductivity required in high temperature solid oxide fuel cell (SOFC) applications has led to the investigation of the substitutionally-mixed (La, Sr) (Cr, Mn)O<sub>3</sub> [1] and (La, Ca) (Cr, Co)O<sub>3</sub> [2] systems. LaCrO<sub>3</sub> and LaCoO<sub>3</sub> belong to a class of materials known as pseudo-perovskites. The basic perovskite structure is represented by the formula ABO<sub>3</sub> in which A, the large cation site, may be an alkali, alkaline earth or rare earth ion, and B represents a transition metal cation. This system involves pseudo-perovskites because their structures deviate from the ideal cubic perovskite structure (i.e. rhombohedral and orthorhombic). This system involves compounds prepared with both Cr to Co B-site ions in an attempt to retain in the compounds the desirable properties found in the end members (e.g. LaCoO<sub>3</sub>—high conductivity and sinterability, LaCrO<sub>3</sub>—chemical stability). Ca is also substituted as an acceptor to the parent La A-site cations in order to increase the small polaron carrier concentration found on the B-site cations in accordance with the Verwey controlled ionic valency principle [3]. Ca also enhanced the sinterability of compounds [4].

LaCrO<sub>3</sub> exhibits a thermally-activated high temperature electrical conductivity due to p-type small polaron hopping among the B-site cations and is stable to high temperatures over a wide range of oxygen partial pressures. LaCoO<sub>3</sub> apparently conducts via the same mechanism as LaCrO<sub>3</sub> but with a significantly greater conductivity.

Our recent results on La<sub>1-x</sub>Ca<sub>x</sub>Cr<sub>1-y</sub>Co<sub>y</sub>O<sub>3</sub> have shown that the compositions with 0.1 < x < 0.3 and

0.1 < y < 0.3 can be sintered to densities above 94% theoretical density (TD) in air at 1400 °C and below. The improvements in densification resulted from the formation of a transient liquid phase. The composition of the liquid phase was dependent upon the amount of Co and Ca substitution. The liquid phase dispersed along the grain boundaries and formed the solid solution with the parent structure. Therefore, it did not alter the chemical stability of the materials if the Co substitution for Cr was kept lower than 30 mol %; otherwise, the stability against reduction at high temperature was diminished [2]. It was therefore desirable to investigate the electrical properties of solid solutions of (La,Ca) (Cr,Co)O<sub>3</sub>.

The objectives of the present investigation are to provide data on electrical conductivity and Seebeck coefficient for the (La,Ca) (Cr,Co)O<sub>3</sub> system, and to evaluate the results in terms of the small polaron model.

## 2. Experimental procedure

Specimens in the (La, Ca) (Cr, Co)O<sub>3</sub> system were prepared by a polymer precursor method similar to that first described by Pechini [5]. The starting chemicals were La and Ca carbonates and Cr and Co nitrates. All chemicals were reagent grade materials and were standardized by thermogravimetric methods to determine the actual cation contents. The desired compositions were prepared by dissolving measured amounts of selected carbonates and nitrates in solutions of citric acid, ethylene glycol and water. The mixtures were heated on a hot plate at about 95 °C until polymerization had occurred. Subsequent heat-

ting at higher temperatures resulted in the decomposition of the polymer resin and allowed conversion into the desired oxide. Final calcination was carried out at 850 °C for 8 h. The resulting powders were milled and subjected to X-ray diffraction to ensure that they were single phase. The powders were pressed into bars with the aid of PVA and water binder; compaction pressure of 2500 kg cm<sup>-2</sup> yielded 0.6 × 0.4 × 3.0 cm bars with density of 52% of theoretical. Densification was conducted at 1400 °C for 10 h in a SiC heated box furnace. Bulk densities of compositions measured by the liquid (Freon) displacement technique were about 96% of theoretical.

Electrical conductivity and thermoelectric power measurements were made simultaneously in an apparatus which could measure three samples at a time. For these measurements the samples were cut into bars of dimensions 0.3 × 0.3 × 2.0 cm and electroded with Pt paste. The specimens were mounted between two platinum blocks, which had Pt-10% Rh/Pt thermocouples as electrical contacts. Pt wire heater was wound on the lower end of the holder to generate the temperature gradient along the vertical direction. Three sets of specimens and holders were contained in Al<sub>2</sub>O<sub>3</sub> tubes within a MoSi furnace, where temperature was controlled by a Eurotherm temperature controller. The Seebeck coefficient was determined by measuring temperature gradients and thermal EMFs through the common leads of the thermocouples. Electrical conductivity measurements were made using the two-probe, four-wire Kelvin technique in which two leads carry the test signal (1 mA) and the other two measure the voltage drop. The measurements were made using a data logger (Hewlett Packard 3497A data acquisition/control unit) which employs an HP-85 computer both as a control and read-out device. More details on this apparatus are available in Reference 6.

### 3. Results and discussion

Conduction in LaCrO<sub>3</sub> and LaCoO<sub>3</sub> is thought to occur by the diffusion of p-type small polarons among Cr or Co ions. A polaron is associated with a particular Cr or Co site if the ion is in the +4 valence state, rather than the stoichiometric +3 valence state. The polaron hopping is characterized by a thermally activated mobility. When the concentration of small polarons is independent of temperature, the high temperature conductivity is expected to take the form

$$\sigma = A/T^s \exp(-E_a/kT) \quad (1)$$

where  $A$  is both a charge carrier concentration and material constant,  $T$  is the absolute temperature,  $s = 1$  in the adiabatic limit and  $s = 3/2$  in the non-adiabatic regime,  $E_a$  is the activation energy, and  $k$  is the Boltzmann constant. Therefore, for materials which obey the small polaron mechanism, Arrhenius plots are expected to be linear, with a slope proportional to the activation energy associated with small polaron hops. For this study, the adiabatic form was used to analyse the conductivity data. It has been determined that this is the correct form for LaCrO<sub>3</sub> [7].

The electrical conductivity data for LaCr<sub>1-y</sub>Co<sub>y</sub>O<sub>3</sub> are shown in Fig. 1, as log( $\sigma$ ) as a function of reciprocal temperature. As can be seen, the electrical conductivity increases with increasing temperature and Co content. Fig. 2 shows the electrical conductivity at 1000 °C plotted as a function of Co content. The electrical conductivity at 1000 °C increases slowly when the Co content is less than 50 mol %, after which it increases sharply with further increase in Co content, indicating a sharp increase in the mobility or carrier concentration. The electrical conductivity is also plotted according to the small polaron model as log( $\sigma T$ ) versus reciprocal temperature in Fig. 3. The end members of the series, LaCrO<sub>3</sub> and LaCoO<sub>3</sub>, exhibit small polaron behaviour over a wide temperature range (see Fig. 3) and have very similar activation energies. The conductivity of undoped LaCoO<sub>3</sub> is about 200 times greater than that of LaCrO<sub>3</sub>. A least squares fit to the data gives an activation energy of 0.18 eV for LaCrO<sub>3</sub> and 0.25 eV for LaCoO<sub>3</sub>. The linearity of the data for the end members over such an extended temperature range is consistent with the earlier identification of the conductivity in these materials as being due to a temperature-independent concentration of p-type small polarons [7, 8]. In spite of the larger intrinsic electronic conductivity of LaCoO<sub>3</sub>, a small substitution of Co for Cr in LaCrO<sub>3</sub>

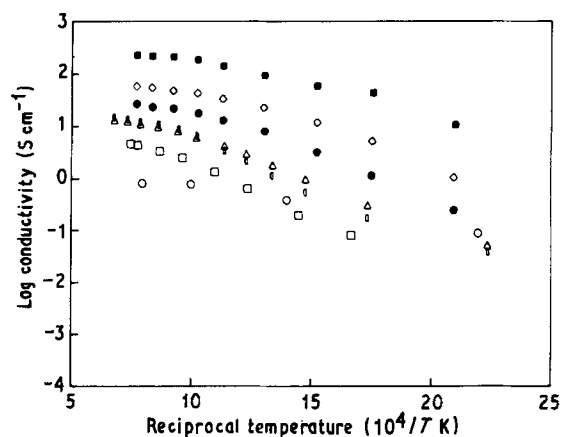


Figure 1 Electrical conductivity of LaCr<sub>1-y</sub>Co<sub>y</sub>O<sub>3</sub> as a function of Co content and temperature. ○,  $y = 0.0$ ; □,  $y = 0.1$ ; △,  $y = 0.2$ ; ◇,  $y = 0.3$ ; ●,  $y = 0.5$ ; ◆,  $y = 0.7$ ; ■,  $y = 1.0$ .

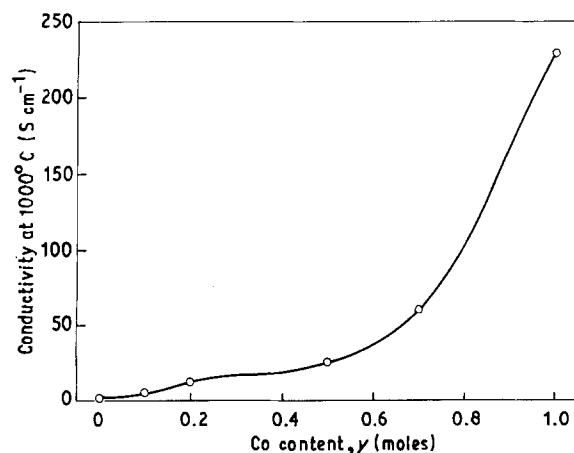


Figure 2 Electrical conductivity at 1000 °C as a function of Co content.

results in a sharp drop in low temperature conductivity from that exhibited by either end member (see Fig. 1). This minimum, which at room temperature is more than three orders of magnitude below that of  $\text{LaCrO}_3$ , occurs at a Co concentration of 10 mol %. In addition, these small substitutions of Co result in a non-linear temperature dependence with increased slope. The maximum slope observed occurs in the 10 mol % Co composition and corresponds to an activation energy of 0.47 eV. As can be seen from Fig. 4, the activation energy increases with Co content to a maximum at 10 mol % and then linearly decreases as Co content increases. The substitution of small amounts of Co for Cr has been found to cause the room temperature electrical conductivity to drop orders of magnitude below that of either end member and increase in activation energy. This behaviour is attributed to a lower small polaron site energy at the Co sites as compared to Cr sites. The lower energy Co sites act as traps for carriers diffusing among Cr sites. Therefore, the activation energy for conduction is increased from that of  $\text{LaCrO}_3$ . At higher Co concentrations, direct transport among Co sites becomes possible and the conductivity increases and activation energy decreases.

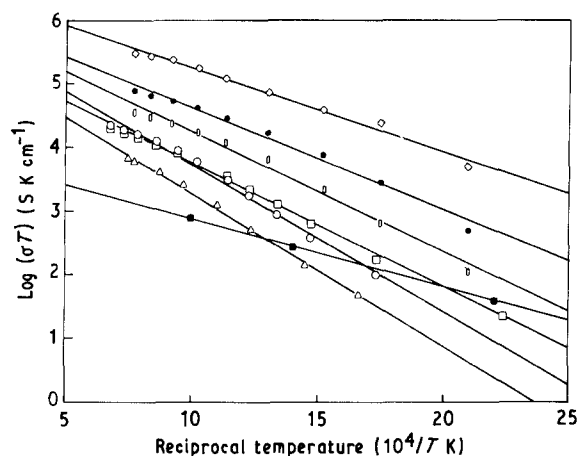


Figure 3 Log  $(\sigma T)$  versus reciprocal temperature for  $\text{LaCr}_{1-y}\text{Co}_y\text{O}_3$ . (The solid lines are calculated by the least squares method.) ■,  $y = 0.0$ ; △,  $y = 0.1$ ; ○,  $y = 0.2$ ; □,  $y = 0.3$ ; ○,  $y = 0.5$ ; ●,  $y = 0.7$ ; ◇,  $y = 1.0$ .

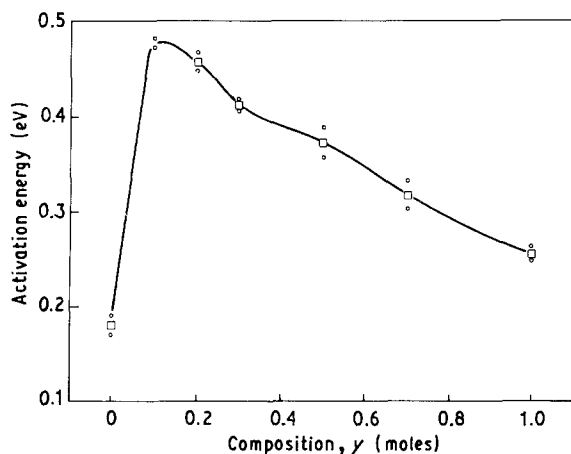


Figure 4 Activation energy for conductivity versus Co content.

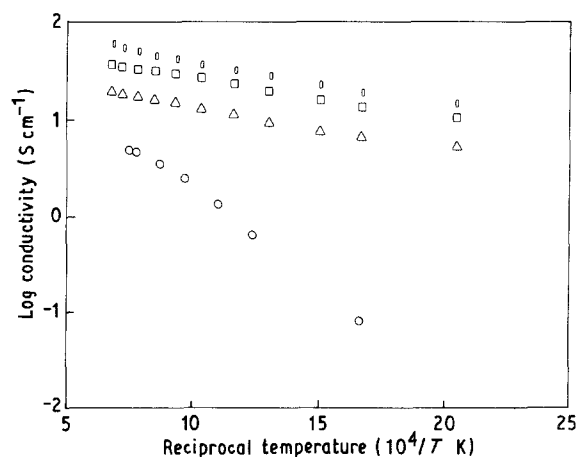


Figure 5 Electrical conductivity of  $\text{La}_{1-x}\text{Ca}_x\text{Cr}_{0.9}\text{Co}_{0.1}\text{O}_3$  as a function of Ca content and temperature. ○,  $x = 0.0$ ; △,  $x = 0.1$ ; □,  $x = 0.2$ ; ◇,  $x = 0.3$ .

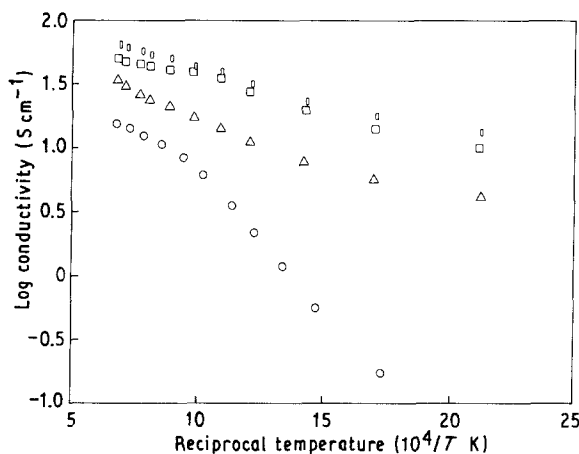


Figure 6 Electrical conductivity of  $\text{La}_{1-x}\text{Ca}_x\text{Cr}_{0.8}\text{Co}_{0.2}\text{O}_3$  as a function of Ca content and temperature. ○,  $x = 0.0$ ; △,  $x = 0.1$ ; □,  $x = 0.2$ ; ◇,  $x = 0.3$ .

The electrical conductivity data for  $\text{La}_{1-x}\text{Ca}_x\text{Cr}_{0.9}\text{Co}_{0.1}\text{O}_3$ ,  $\text{La}_{1-x}\text{Ca}_x\text{Cr}_{0.8}\text{Co}_{0.2}\text{O}_3$  and  $\text{La}_{1-x}\text{Ca}_x\text{Cr}_{0.7}\text{Co}_{0.3}\text{O}_3$  (with  $x = 0.1, 0.2$  and  $0.3$ ) are shown in Figs 5, 6 and 7, respectively, as log  $(\sigma)$  as a function of reciprocal temperature. Figs 8, 9 and 10 show the same data plotted as log  $(\sigma T)$  versus reciprocal temperature; these plots show that the conductivity obeys the small polaron mechanism. Activation energies for hopping were calculated from Figs 8, 9 and 10 and plotted in Fig. 11, as a function of Ca content. As can be seen with Ca content of 10–30 mol %, all three Co content levels have essentially the same activation energy. The additional substitution of Ca for La in  $\text{La}(\text{Cr}, \text{Co})\text{O}_3$  eliminated the increase in activation energy that was observed with Co substitution for Cr. The substitution of 10 mol % Ca for La in the  $\text{La}(\text{Cr}, \text{Co})\text{O}_3$  series increased the conductivity in  $\text{LaCrO}_3$  by approximately 10% which was anticipated in view of a carrier density increase of 10% in accordance with Verwey's principle. As in the case of  $\text{La}_{1-x}\text{Ca}_x\text{CrO}_3$  and  $\text{La}_{1-x}\text{Ca}_x\text{CoO}_3$ , the substitution of Ca for La in  $\text{LaCr}_{1-y}\text{Co}_y\text{O}_3$  should result in the formation of  $\text{Cr}^{4+}$  and  $\text{Co}^{4+}$  in order to preserve the electrical neutrality. Formation of both  $\text{Cr}^{4+}$  and  $\text{Co}^{4+}$  increases the

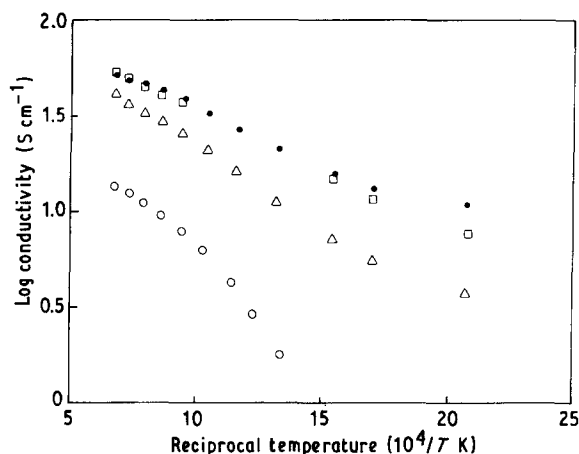


Figure 7 Electrical conductivity of  $\text{La}_{1-x}\text{Ca}_x\text{Cr}_{0.7}\text{Co}_{0.3}\text{O}_3$  as a function of Ca content and temperature.  $\circ$ ,  $x = 0.0$ ;  $\triangle$ ,  $x = 0.1$ ;  $\square$ ,  $x = 0.2$ ;  $\bullet$ ,  $x = 0.3$ .

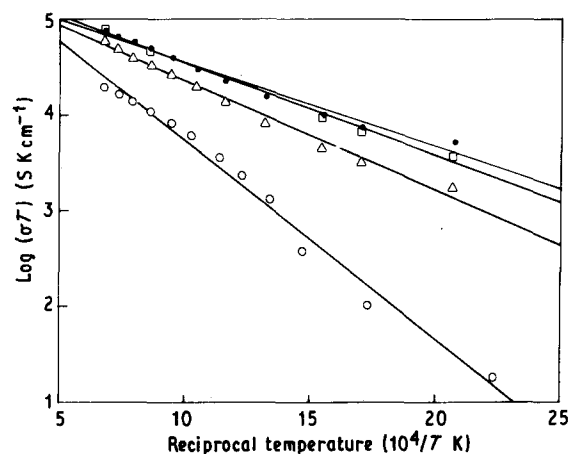


Figure 10  $\text{Log } (\sigma T)$  versus reciprocal temperature for  $\text{La}_{1-x}\text{Ca}_x\text{Cr}_{0.7}\text{Co}_{0.3}\text{O}_3$ . (The solid lines are calculated by the least squares method.)  $\circ$ ,  $x = 0.0$ ;  $\triangle$ ,  $x = 0.1$ ;  $\square$ ,  $x = 0.2$ ;  $\bullet$ ,  $x = 0.3$ .

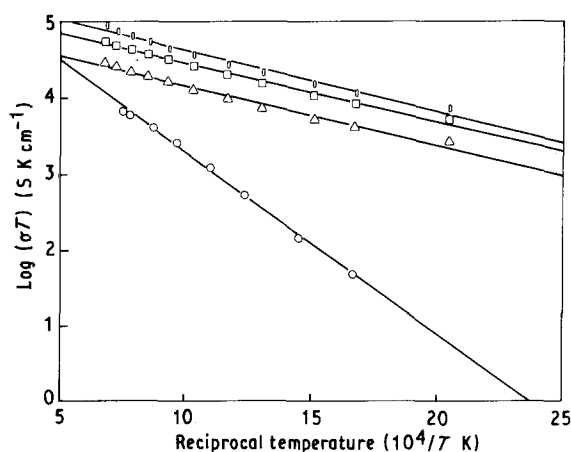


Figure 8  $\text{Log } (\sigma T)$  versus reciprocal temperature for  $\text{La}_{1-x}\text{Ca}_x\text{Cr}_{0.9}\text{Co}_{0.1}\text{O}_3$ . (The solid lines are calculated by the least squares method.)  $\circ$ ,  $x = 0.0$ ;  $\triangle$ ,  $x = 0.1$ ;  $\square$ ,  $x = 0.2$ ;  $\bullet$ ,  $x = 0.3$ .

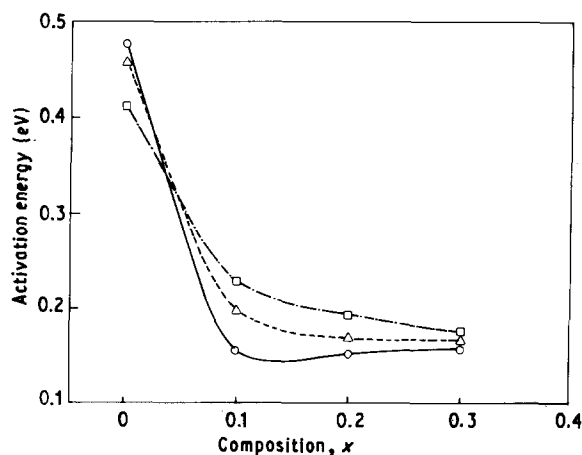


Figure 11 Activation energy for conductivity versus Ca content for  $\text{La}_{1-x}\text{Ca}_x\text{Cr}_{1-y}\text{Co}_y\text{O}_3$ .  $\circ$ ,  $y = 0.1$ ;  $\triangle$ ,  $y = 0.2$ ;  $\square$ ,  $y = 0.3$ .

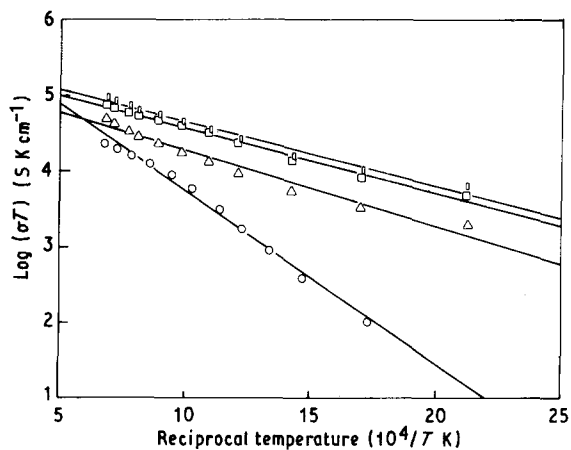


Figure 9  $\text{Log } (\sigma T)$  versus, reciprocal temperature for  $\text{La}_{1-x}\text{Ca}_x\text{Cr}_{0.8}\text{Co}_{0.2}\text{O}_3$ . (The solid lines are calculated by the least squares method.)  $\circ$ ,  $x = 0.0$ ;  $\triangle$ ,  $x = 0.1$ ;  $\square$ ,  $x = 0.2$ ;  $\bullet$ ,  $x = 0.3$ .

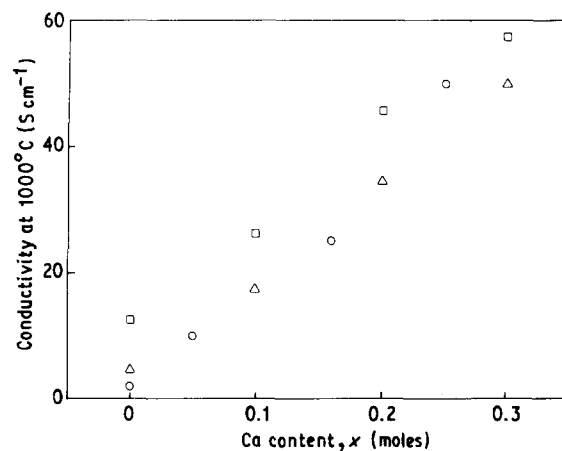


Figure 12 Electrical conductivity at  $1000^\circ\text{C}$  as a function of Ca content for  $\text{La}_{1-x}\text{Ca}_x\text{Cr}_{1-y}\text{Co}_y\text{O}_3$ .  $\circ$ ,  $y = 0.0$ ;  $\triangle$ ,  $y = 0.1$ ;  $\square$ ,  $y = 0.2$ .

small-polaron concentration and decreases the activation energy for conduction. Fig. 12 shows the electrical conductivity at  $1000^\circ\text{C}$  as a function of Ca content in  $\text{La}_{1-x}\text{Ca}_x\text{Cr}_{0.9}\text{Co}_{0.1}\text{O}_3$  and  $\text{La}_{1-x}\text{Ca}_x\text{Cr}_{0.8}\text{Co}_{0.2}\text{O}_3$ . The electrical conductivity at  $1000^\circ\text{C}$  as a function of Ca in  $\text{La}_{1-x}\text{Ca}_x\text{CrO}_3$  is included in Fig. 12 from

Reference 9 for comparison. As can be seen, the electrical conductivity of  $\text{La}_{1-x}\text{Ca}_x\text{Cr}_{0.9}\text{Co}_{0.1}\text{O}_3$  and  $\text{La}_{1-x}\text{Ca}_x\text{Cr}_{0.8}\text{Co}_{0.2}\text{O}_3$  at  $1000^\circ\text{C}$  is slightly higher than that of  $\text{La}_{1-x}\text{Ca}_x\text{CrO}_3$ . This is probably due to a higher small polaron concentration in Co-containing compositions. A possible explanation for this involves considering the different spin states of  $\text{Co}^{3+}$ . The low spin ( $S = 0$ ) state is the most stable and predominates

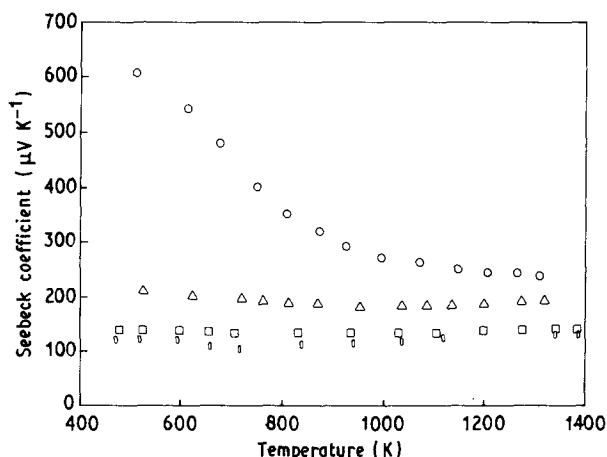


Figure 13 Seebeck coefficients of  $\text{La}_{1-x}\text{Ca}_x\text{Cr}_{0.9}\text{Co}_{0.1}\text{O}_3$  as a function of Ca content and temperature.  $\circ$ ,  $x = 0.0$ ;  $\triangle$ ,  $x = 0.1$ ;  $\square$ ,  $x = 0.2$ ;  $\square$ ,  $x = 0.3$ .

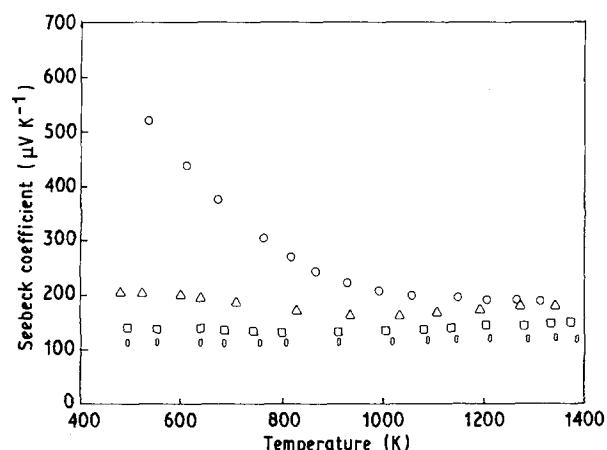


Figure 14 Seebeck coefficients of  $\text{La}_{1-x}\text{Ca}_x\text{Cr}_{0.8}\text{Co}_{0.2}\text{O}_3$  as a function of Ca content and temperature.  $\circ$ ,  $x = 0.0$ ;  $\triangle$ ,  $x = 0.1$ ;  $\square$ ,  $x = 0.2$ ;  $\square$ ,  $x = 0.3$ .

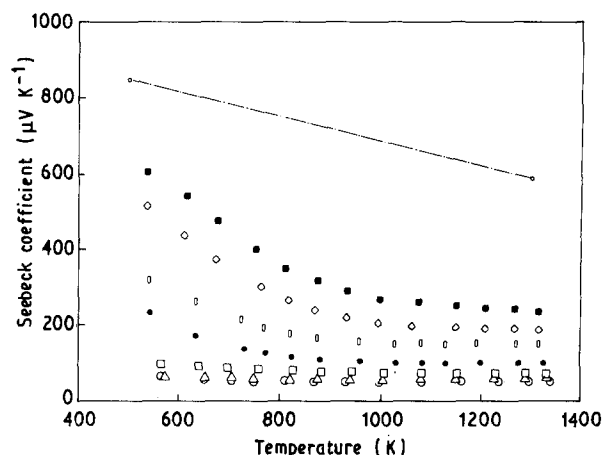


Figure 15 Seebeck coefficients of  $\text{LaCr}_{1-y}\text{Co}_y\text{O}_3$  as a function of Co content and temperature.  $\circ$ ,  $y = 1.0$ ;  $\triangle$ ,  $y = 0.9$ ;  $\square$ ,  $y = 0.7$ ;  $\bullet$ ,  $y = 0.5$ ;  $\circ$ ,  $y = 0.3$ ;  $\diamond$ ,  $y = 0.2$ ;  $\blacksquare$ ,  $y = 0.1$ ;  $\square$ ,  $y = 0.0$ .

at low temperature.  $\text{Co}^{4+}$  is not energetically favourable for this state. As the temperature increases, higher spin states of  $\text{Co}^{3+}$  ( $S = 1$ ,  $S = 2$ ) become populated. Therefore, the formation of additional  $\text{Co}^{4+}$  occurs at  $1000^\circ\text{C}$ . It can be concluded that the replacement of some of the  $\text{Cr}^{3+}$  ions in the solid solution with  $\text{Co}^{3+}$

ions enables the magnitude of the electrical conductivity to be controlled at low Co concentration.

Thermopower measurements were made to determine the type and concentration of charge carriers. Figs 13–15 show Seebeck coefficient plotted as a function of temperature for  $\text{La}_{1-x}\text{Ca}_x\text{Cr}_{0.9}\text{Co}_{0.1}\text{O}_3$ ,  $\text{La}_{1-x}\text{Ca}_x\text{Cr}_{0.8}\text{Co}_{0.2}\text{O}_3$  and  $\text{LaCr}_{1-y}\text{Co}_y\text{O}_3$ , respectively. (In Fig. 15, the dotted line is taken from Reference 10 for comparison.) In  $\text{LaCr}_{1-y}\text{Co}_y\text{O}_3$ , the substitution of Co for Cr significantly decreased the Seebeck coefficient, indicating that Co substitution for Cr increases the carrier concentration. As the Co content increased, the Seebeck coefficient was independent of temperature, indicating that the carrier mobility, rather than carrier concentration, was thermally activated. According to Heikes's formula this type of behaviour indicates a small polaron conduction mechanism which agrees with the electrical conductivity measurements. In the cases of  $\text{La}_{1-x}\text{Ca}_x\text{Cr}_{0.9}\text{Co}_{0.1}\text{O}_3$  and  $\text{La}_{1-x}\text{Ca}_x\text{Cr}_{0.8}\text{Co}_{0.2}\text{O}_3$ , introduction of Ca significantly decreased the Seebeck coefficient and resulted in a temperature-independent Seebeck coefficient.

The site occupancy,  $\kappa$ , of a small polaronic conductor with energetically degenerate sites can be determined by using the Seebeck coefficient and applying Heikes's formula,

$$Q = (k/e) \{ \ln[1 - \kappa]/\kappa \} + Q^*/k \quad (2)$$

where  $k$  is the Boltzmann constant,  $e$  is the unit charge,  $\kappa$  is the fraction of hopping sites which are occupied and  $Q^*$  is the vibrational entropy per charge carrier, estimated to be  $< 10 \mu\text{V K}^{-1}$  and neglected in these calculations. Thus, Heikes's formula implies a temperature-independent Seebeck coefficient for constant  $\kappa$ . Plots of Seebeck coefficient versus temperature (Figs 13–15) indicated that  $\kappa$  was not constant for compositions at the lower measurement temperatures and low Co concentrations. Using the Seebeck data and Heikes's formula, the fraction of hopping sites at  $1000^\circ\text{C}$  was calculated as a function of Co content (Fig. 16). As can be seen, the fraction of occupied hopping sites increased as a function of Co. This behaviour agreed with the electrical conductivity.

In  $\text{La}_{1-x}\text{Ca}_x\text{Cr}_{0.9}\text{Co}_{0.1}\text{O}_3$  and  $\text{La}_{1-x}\text{Ca}_x\text{Cr}_{0.8}\text{Co}_{0.2}\text{O}_3$ , introduction of Ca decreased the Seebeck coefficient and resulted in a temperature-independent behaviour. The Seebeck coefficient of compositions did not change significantly as a function of Co once Ca was substituted for La. Therefore, the Seebeck coefficient of compositions  $\text{La}_{1-x}\text{Ca}_x\text{Cr}_{0.9}\text{Co}_{0.1}\text{O}_3$  and  $\text{La}_{1-x}\text{Ca}_x\text{Cr}_{0.8}\text{Co}_{0.2}\text{O}_3$  is expected to approach that of  $\text{La}_{1-x}\text{Ca}_x\text{CrO}_3$  with corresponding Ca. Using the Seebeck data and Heikes's formula, the fraction of occupied hopping sites at  $1000^\circ\text{C}$  was calculated for compositions as a function of Ca content (Fig. 17). The fraction of occupied hopping sites significantly increased as Ca was introduced, further increases in Ca smoothly developed the fraction of occupied hopping sites. It is evident that Ca enters the La site as an acceptor, thereby increasing the conductivity, which is consistent with Verwey's controlled ionic valency principle. However, the Seebeck coefficient of com-

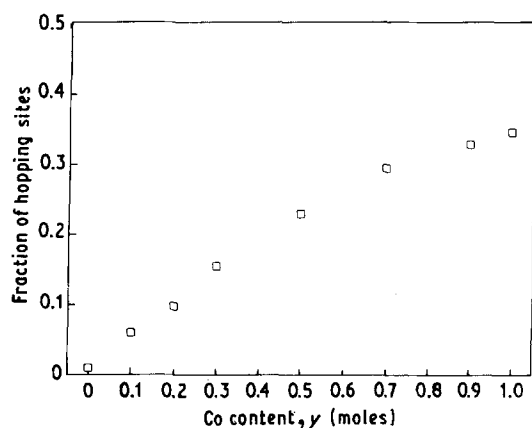


Figure 16 Calculated fraction of occupied hopping sites as a function of Co content at 1000 °C for  $\text{LaCr}_{1-y}\text{Co}_y\text{O}_3$ .

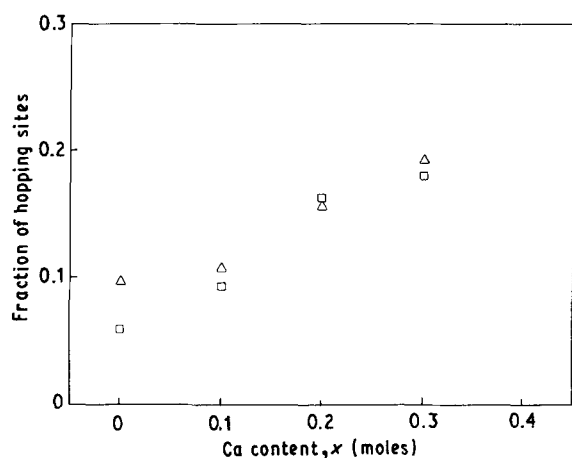


Figure 17 Calculated fraction of occupied hopping sites as a function of Ca content at 1000 °C for  $\text{La}_{1-x}\text{Ca}_x\text{Cr}_{1-y}\text{Co}_y\text{O}_3$ .  $\square$ ,  $y = 0.1$ ;  $\triangle$ ,  $y = 0.2$ .

positions with 30 mol% Co or less in the  $\text{La}(\text{Cr}, \text{Co})\text{O}_3$  series exhibited a Seebeck coefficient approaching that of  $\text{LaCrO}_3$  at low temperatures (around 150 °C). Samples with a higher Co content displayed Seebeck coefficients dependent on Co concentration ( $Q$  decreased as the mol % Co increased.)

#### 4. Conclusion

The electrical conductivity as measured in air from 100 to 1100 °C increased with increasing Co and Ca content. At 1000 °C, values from  $1.5 \text{ S cm}^{-1}$  (for  $\text{LaCr}_{0.9}\text{Co}_{0.1}\text{O}_3$ ) to  $50 \text{ S cm}^{-1}$  (for  $\text{La}_{0.7}\text{Ca}_{0.3}\text{Cr}_{0.9}\text{Co}_{0.1}\text{O}_3$ ) were measured. The Seebeck coefficients were positive, indicating p-type conductivity. The substitution of Co for Cr significantly decreased the Seebeck coefficients, indicating that Co substitution for Cr increased the carrier concentration. Additional Ca substitution for La resulted in a further decrease in the Seebeck coefficient. Seebeck coefficients then exhibited a temperature-independent behaviour, indicating that the carrier mobility, rather than carrier concentration, was thermally activated.

#### Acknowledgements

This research was sponsored by the US Department of Energy, Basic Science Division. Rasit Koc also received partial support from the Turkish Ministry of Education.

#### References

1. R. KOC, H. U. ANDERSON, S. A. HOWARD and D. M. SPARLIN, in *Proceedings of the First International Symposium on Solid Oxide Fuel Cells*, Florida, October 1989, (edited by S. C. Singhal) p. 220.
2. R. KOC, PhD thesis, University of Missouri, Rolla (1989).
3. E. J. VERWEY, P. W. HAAIJAM, F. C. ROMEIJH and G. W. VAN OOSTERHOUT, *Phillips Res. Report* **5** (1950) 173.
4. R. KOC and H. U. ANDERSON, *Ceram. Trans.* **12** (1990) 659.
5. M. PECHINI, US Patent 3 330 697, (1967).
6. G. GARINI, MS thesis, University of Missouri, Rolla (1988).
7. B. K. FLANDERMEYER, PhD thesis, University of Missouri, Rolla (1984).
8. H. OHBAYASHI, T. KUDO and T. GEJO *J. Appl. Phys.* **37** (1966) 1424.
9. S. SONG, M. YOSHIMURA and S. SOMIYA *J. Mater. Sci. Soc. Jpn.* **19** (1982) 49.
10. D. P. KARIM and A. T. ALDRED *Phys. Rev. B* **20** (1979) 2255.

Received 17 June

and accepted 25 November 1991